Waste iron-based disposable chemical warmer derived electrocatalyst for water splitting

Keyru Serbara Bejigo[1], Raaju Sundhar Arul Saravanan[1], Kousik Bhunia[1], Sang-Jae Kim[1,2,3*]

[1]Nanomaterials & System Lab, Major of Mechatronics Engineering, Faculty of Applied Energy System, Jeju National University, Jeju 63243, Republic of Korea

[2]Nanomaterials & System Lab, Major of Mechanical System Engineering, College of Engineering, Jeju National University, Jeju 63243, Republic of Korea.

[3]Research Institute of New Energy Industry (RINEI), Jeju National University, Jeju 63243, Republic of Korea

[*]Corresponding author. Email address: kimsangj@jejunu.ac.kr

Materials and reagents

Used CHP was obtained from a chemical disposal container in Korea. We bought hydrochloric acid (HCl), Hexamethylenetetramine (HMT), potassium hydroxide (KOH, 85 %) and Nafion (5 wt%) from Sigma Aldrich. The fuel cell store in Korea provided carbon black (Vulcan XC 72), carbon-supported platinum (30 wt%), and ruthenium oxide. We used double-distilled water for the experiments and analysis. We used reagents of analytical grade and didn't perform any further purification.

Instrumentation

XRD patterns were acquired from an X-ray Powder Diffractometer (Malvern Panalytical, Malvern, UK) instrument. The degree of carbonization was assessed through Raman spectroscopy using Raman spectrometers (Horiba Jobin-Yvon, France) that featured an argon-ion laser with an excitation wavelength of 514 nm and covered a Raman shift range of 1150-1750 cm^{-1}. Field emission scanning electron microscopy (FESEM, MIRA3) and field emission transmission electron microscopes (TEM, JEOL, JEM-2100F) were used to examine the morphology and structure of the samples. An XPS analysis was carried out using X-ray photoelectron spectroscopy (XPS, VG Escalab 250) using Al-Kα radiation at Busan KBSI. The Brunauer-Emmett-Teller (BET) surface area analysis was performed using the BELSORP MINI X and Microtrac MRB Chem BET analyzer. The iron concentration was analyzed by an Inductively coupled plasma-optical Emission Spectrometer (AVIO 550). In preparation for ICP-OES analysis, the digested sample was diluted to a concentration within the instrument's accurate detection limits. The actual concentration of the sample was then determined by multiplying the value obtained from ICP-OES by the dilution factor.

Electrochemical measurements

A commercial Pt/C catalyst (30%) was employed as a reference catalyst for HER, whereas ruthenium oxide (RuO_2) was utilized for the OER. The electrochemical impedance spectroscopy (EIS) was recorded at applied potentials of 1.53 V *vs*. RHE for OER in the frequency range from 10^{-2} to 10^5 Hz. Tafel slopes for OER and HER were determined by plotting the overpotential (η) against the logarithm of current density using polarization curves. All potentials were converted to RHE from Ag/AgCl without resistance compensation by the following equation $E_{RHE} = E_{(Ag/AgCl)} + 0.059\ pH + E°_{(Ag/AgCl)}$.

The water drainage method was used to measure the H_2 and O_2 gases produced in the bifunctional Fe/Fe_3O_4/NC water electrolyzer. The setup follows an H-cell configuration, with both compartments separated by a Fumasep membrane. A constant current density of 50 mA cm^{-2} was applied. Faradic Efficiency (η) was estimated based on the following equation.

$$\eta_{eff} = \frac{V_{exp.}}{V_{theor.}}$$

V exp. The measured gas volume at 273.15 K and 105 Pa.

$V_{theor.}$ is calculated by using the equation

$$\eta_{theor.} = \frac{I.t.Vs}{n.F}$$

In this equation, *I, t, Vs, n*, and *F* stand for applied current (A), total water splitting time (s), standard molar volume (22.4 L mol-1), number of exchanging electrons (n = 4 and 2, respectively, for O_2 and H_2), and Faraday's constant (96484 C mol^{-1}).

We have calculated the percentage of each species of nitrogen present at each catalyst from the spectra area of deconvoluted XPS using XPSPEAK41 software and the total atomic percentage of N in each component using the following equation.

$$\%A = \frac{A_i}{\Sigma A_i}$$

Where A_i is the area of each component in deconvoluted XPS, and $\sum A_i$ is the total peak area of all compositions.

The atomic percentage of each component N (for example, Fe-N_x) is calculated by

Atomic % Fe-Nx= $\%A_{Fe\text{-}Nx}$ *(%N)

%N is the atomic percentage of nitrogen in the composite catalyst, provided in Table S4.

Fig. S 1. Photograph showing the weight measurement of a single discarded heat pack

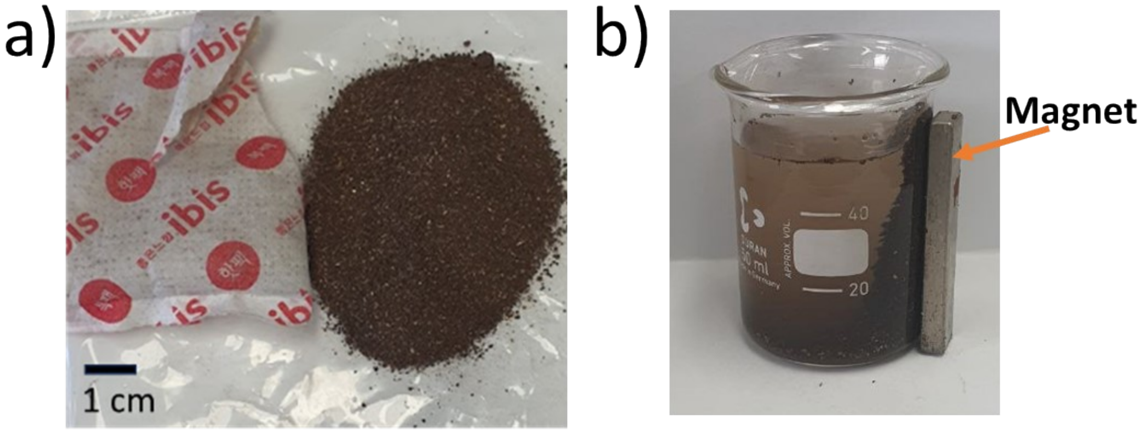

Fig. S 2. Photographs of discarded heat pack at dismantled state (a) and low-gradient magnetic separation (b).

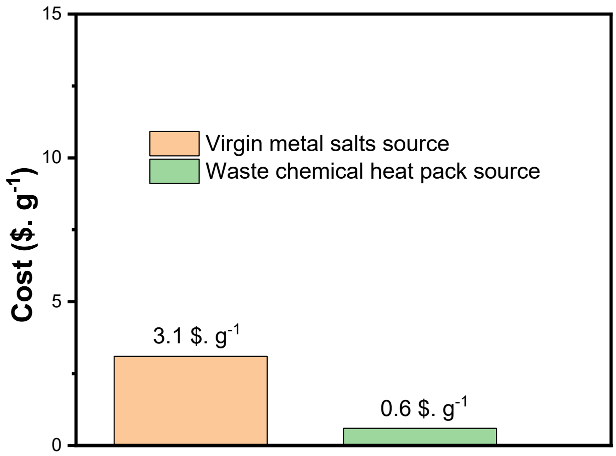

Figure S 3. Cost comparison of Fe/Fe_3O_4/NC from virgin and recycled iron source

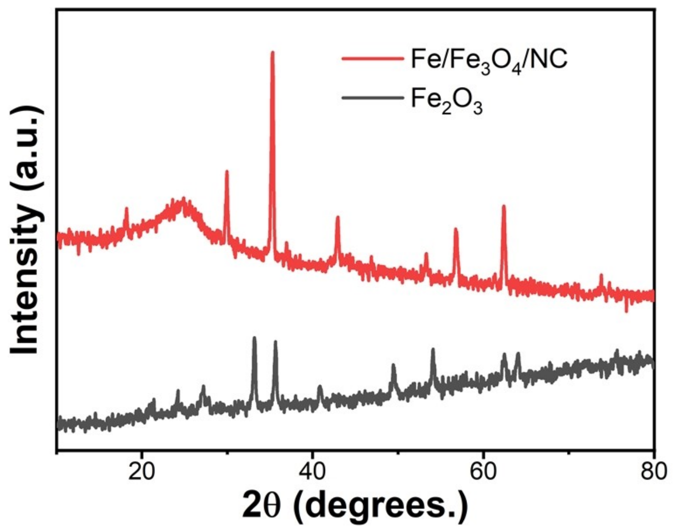

Fig. S 4. XRD patterns of Fe_2O_3 and Fe/Fe_3O_4/NC

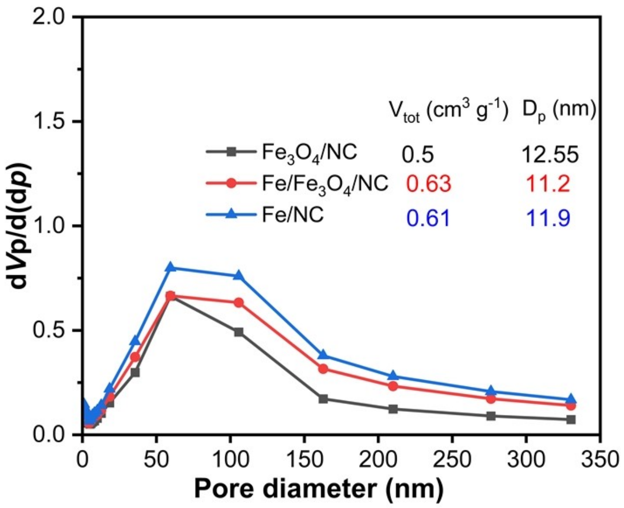

Fig. S 5. Pore size distribution of synthesized catalysts

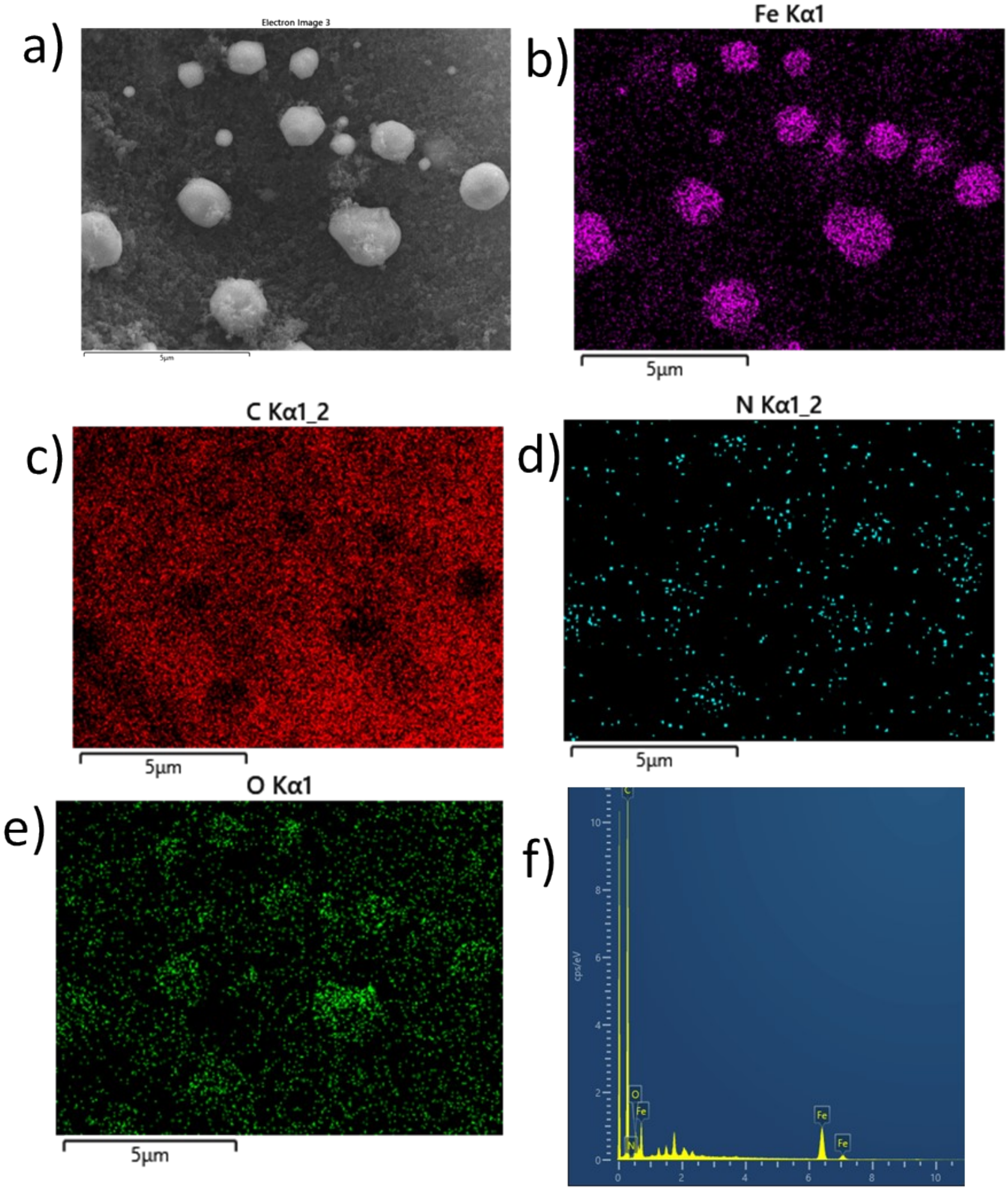

Fig. S 6. SEM image (a), corresponding elemental mapping (b-e) and Energy Dispersive X-ray (EDX) spectra (f) of Fe/Fe_3O_4/NC

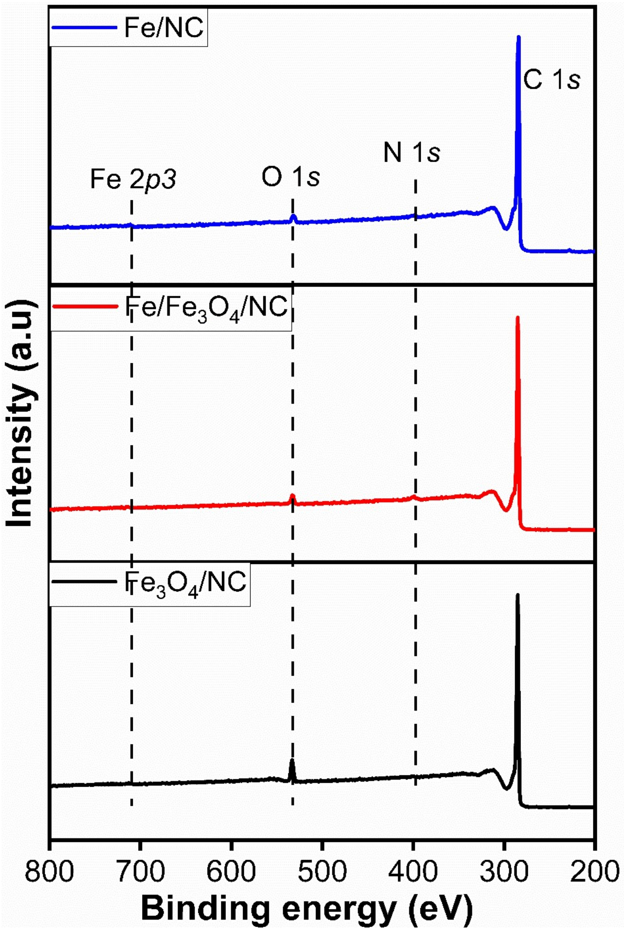

Fig. S 7. XPS survey spectrum of $Fe/Fe_3O_4/NC$ composites.

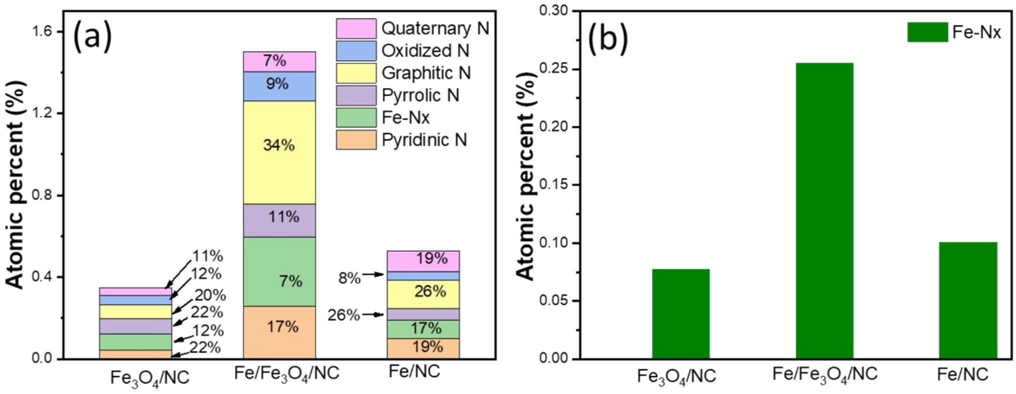

Fig. S 8. Percentages of different N species (b) Atomic percentage of Fe-Nx species in the synthesized catalysts (b)

.

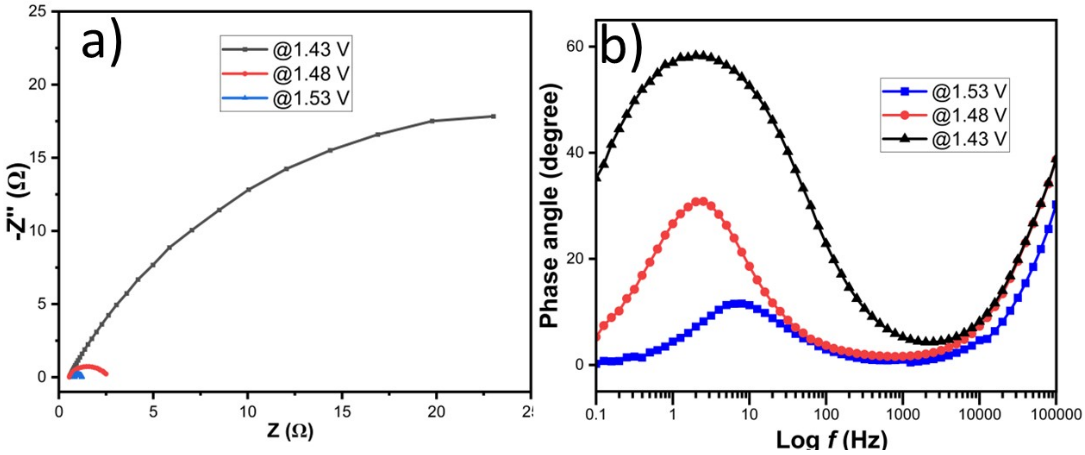

Fig. S 9. EIS spectrum of Fe/Fe_3O_4/NC (850 ºC) measured at different bias potentials (a) and corresponding bode plot (b).

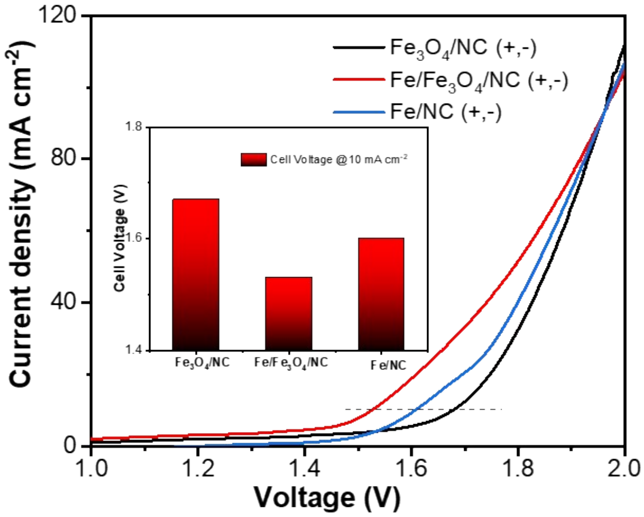

Figure S 10. LSV curves for the water electrolyzer at two-electrode configuration for different bifunctional catalysts at a scan rate of 5.0 mV s^{-1} (inset: cell voltage at 10 mA cm^{-2})

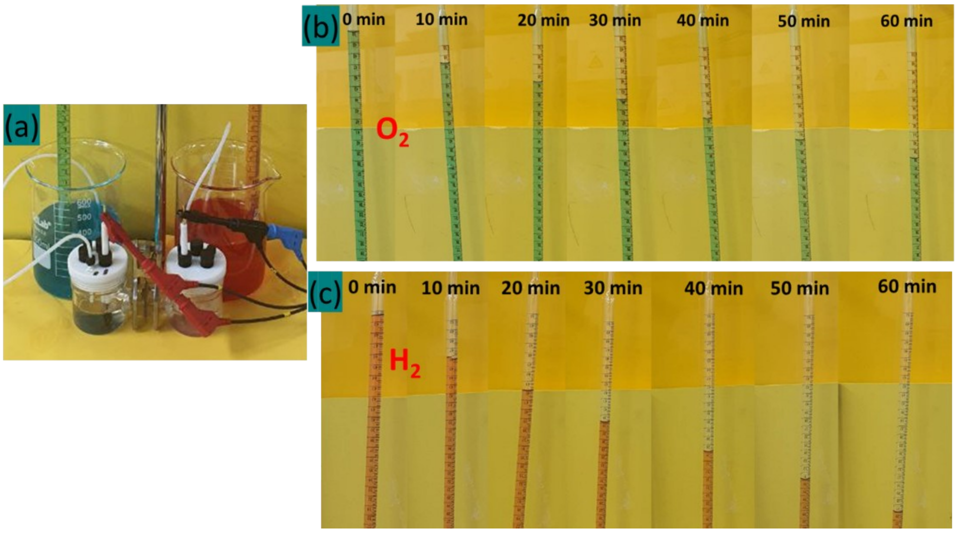

Figure S 11. Photograph of real time H-type cell water electrolyzer setup utilizing Fe/Fe_3O_4/NC bifunctional catalyst (a). The collected oxygen (O_2) and hydrogen (H_2) gases (b and c)

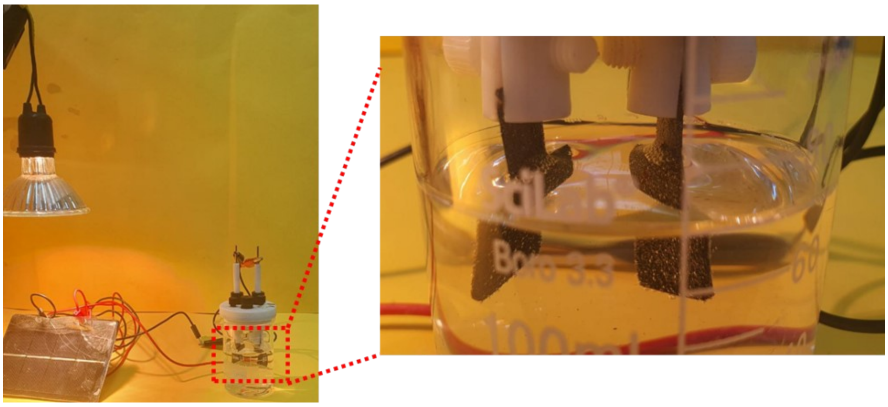

Figure S 12. The water-splitting system powered by a 1.8 V solar cell

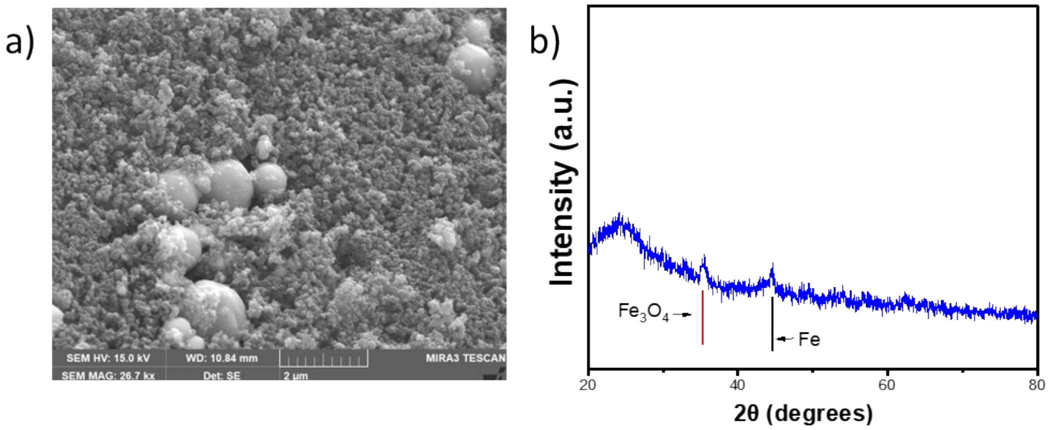

Figure S 13. SEM image (a) and XRD analysis (b) of $Fe/Fe_3O_4/NC$ after stability tests

Table S 1. The synthesis expenses analysis for a 5 g $Fe/Fe_3O_4/NC$ catalyst by using a waste heat pack

<table>
<tr><th>Inputs</th><th>Price</th><th colspan="2">Amount</th><th>Cost</th></tr>
<tr><td>Waste heat pack</td><td>-</td><td colspan="2">1 g</td><td>$ 0.0</td></tr>
<tr><td>Carbon black</td><td>$ 180 per kg</td><td colspan="2">4 g</td><td>$ 0.72</td></tr>
<tr><td>HCl</td><td>$ 60 per L</td><td colspan="2">10 ml</td><td>$ 0.6</td></tr>
<tr><td>HMT</td><td>$40 per kg</td><td colspan="2">4 g</td><td>$ 0.16</td></tr>
<tr><td>Ar</td><td>$ 20 (40 L, 15 MPa)</td><td colspan="2">15 L, 0.1 MPa</td><td>$ 0.1</td></tr>
<tr><td rowspan="3">Electricity</td><td rowspan="3">$ 0.1 per KWh</td><td>Sonication</td><td>1.2 KWh</td><td rowspan="3">13.2 kWh* $ 0.1 KWh^{-1}= $ 1.32</td></tr>
<tr><td>Mixing and drying</td><td>2.0 KWh</td></tr>
<tr><td>Annealing</td><td>10</td></tr>
<tr><td>Total</td><td></td><td colspan="2"></td><td>≈$ 3.0</td></tr>
<tr><td>5 g Pt/C (30%)</td><td></td><td colspan="2"></td><td>$ 598</td></tr>
<tr><td>5 g RuO_2 (99.9%)</td><td></td><td colspan="2"></td><td>$ 451</td></tr>
</table>

Table S 2. The synthesis expenses analysis for a 5 g $Fe/Fe_3O_4/NC$ catalyst by using commercial catalyst source

Inputs	**Price**	**Amount**	**Cost**

$FeCl_3$	$66 per 5 g	1 g		$ 13.4
Carbon black	$ 180 per kg	4 g		$ 0.72
HMT	$40 per kg	4 g		$ 0.16
Ar	$ 20 (40 L, 15 MPa)	15 L, 0.1 MPa		$ 0.1
Electricity	$ 0.1 per KWh	Mixing and drying	2.0 KWh	12.0 kWh* $ 0.1 KWh^{-1}= $1.2
		Annealing	10.0	
Total				≈ $ 15.5

- ✓ The chemical price was obtained from Sigma-Aldrich as of February 2024 (https://www.sigmaaldrich.com/KR/ko) by considering the 99.7% ACS reagent basis for metal salts
- ✓ The electricity price rate was determined by the average price in Korea.
- ✓ Producing the $Fe/Fe_3O_4/NC$ catalyst on a larger scale would lead to a greater reduction in price

Table S3. Physical properties of synthesized $Fe/Fe_3O_4/NC$ composite materials.

Sample	**S_{BET} [a] [$m^2\ g^{-1}$]**	**V_{tot} [b] [$cm^3\ g^{-1}$]**	**D_p [c] (nm)**	**I_D/I_G [d]**
Fe_3O_4/NC	161.7	0.5	12.55	1.11
Fe/Fe_3O_4/NC	223.2	0.63	11.2	1.04
Fe /NC	185.6	0.61	11.9	1.03

a- Surface areas analyzed using the BET method

b- Total pore volumes evaluated from N_2 adsorption isotherms at $P/P_0 = 0.99$.

c- Mesopore diameters evaluated by BJH method from N_2 desorption branches.

d- Raman Intensity peak ratio of I_D and I_G.

Table S4. Surface compositions and corresponding atomic ratios for $Fe/Fe_3O_4/NC$ composites determined from XPS

Sample	C %	Fe %	N%	O
Fe_3O_4/NC	94.26	0.12	0.35	5.27
$Fe/Fe_3O_4/NC$	95.6	0.11	1.5	2.8
Fe/NC	97.38	0.15	0.53	1.94

Table S 5. Comparison of OER, HER and overall water splitting performances for synthesized catalysts, and some recently reported electrocatalysts.

Catalyst	Support	η_{OER} @ *j*=10 mA cm^{-2} [mV]	η_{HER} @ *j*=10 mA cm^{-2} [mV]	Cell voltage @ *j*=10 mA cm^{-2} [V]	Ref.
Fe_3O_4/NC		**270**	**198**	**1.67**	
Fe/Fe_3O_4/NC	**Ni foam (NF)**	**230**	**160**	**1.53**	**This work**
Fe/NC		**240**	**181**	**1.6**	
Cr-Fe_3O_4-N	NF	218	95	1.53	[1]
NiFe-oxide Nanocube		271	197	1.6713	[2]
Fe_3O_4-CoP_x/TiN	Ti foil	331	177	1.75	[3]
Fe_3O_4@graphite	CC	285	121	-	[4]
Fe-CoP/Ti		230	78	1.6	[5]
Fe_3O_4/NCMTs-800(IL)	NF	310	170	1.71	[6]
Al, Fe-CoP/RG	-	280	145	1.66	[7]
CoFe–Se–P	NF	-	183.1	1.59	[8]
Fe-doped $CoWO_4$	NF	259	118	1.55	[9]
$Fe_{0.25}$-CoP	-	262	111	1.57	[9]
CoFeP	NF	350	177	1.57	[10]
Mn-FeP/$Co_3(PO_4)_2$	CC	237	85	1.61	[11]
CoFeN x HNAs/NF	NF	200	259/50 mA/cm^{-2}	1.59	[11]
CoFe/Co-BF	Bamboo fiber	250	46	1.55	[13]
$FeCoS_2$/Co_4S_3/NGF	Graphene foam	276	170	1.68	[14]
Ru-Fe_3O_4/IF	Iron foam	297	128	1.521	[12]
$Bi_3(FeO_4)(MoO_4)_2$		266	199	1.67	[13]

References

1 S. Meng, S. Sun, Y. Liu, Y. Lu and M. Chen, *J. Colloid Interface Sci.*, 2022, **624**, 433–442.

2 A. Kumar and S. Bhattacharyya, *ACS Appl. Mater. Interfaces*, 2017, **9**, 41906–41915.

3 B. Guo, J. Sun, X. Hu, Y. Wang, Y. Sun, R. Hu, L. Yu, H. Zhao and J. Zhu, *ACS Appl. Nano Mater.*, 2019, **2**, 40–47.

4 R. Atchudan, T. N. J. Immanuel Edison, S. Perumal, R. Vinodh, N. Muthuchamy and Y. R. Lee, *Fuel*, 2020, **277**, 118235.

5 C. Tang, R. Zhang, W. Lu, L. He, X. Jiang, A. M. Asiri and X. Sun, *Adv. Mater.*, DOI:10.1002/adma.201602441.

6 G. Liu, B. Wang, P. Ding, Y. Ye, W. Wei, W. Zhu, L. Xu, J. Xia and H. Li, *J. Alloys Compd.*, 2019, **797**, 849–858.

7 S. F. Zai, Y. T. Zhou, C. C. Yang and Q. Jiang, *Chem. Eng. J.*, 2021, **421**, 127856.

8 L. He, B. Cui, B. Hu, J. Liu, K. Tian, M. Wang, Y. Song, S. Fang, Z. Zhang and Q. Jia, *ACS Appl. Energy Mater.*, 2018, **1**, 3915–3928.

9 Q. Yang, H. Dai, W. Liao, X. Tong, Y. Fu, M. Qian and T. Chen, *Dalton Trans.*, 2021, **50**, 18069–18076.

10 L. Ji, J. Wang, X. Teng, T. J. Meyer and Z. Chen, *ACS Catal.*, 2020, **10**, 412–419.

11 D. Li, Y. Xing, R. Yang, T. Wen, D. Jiang, W. Shi and S. Yuan, *ACS Appl. Mater. Interfaces*, 2020, acsami.0c05219.

12 L. Ai, M. Chen, Y. Luo, Y. Tian, X. Wang, W. Wei and J. Jiang, *Colloids Surf. A Physicochem. Eng. Asp.*, 2022, **651**, 129767.

13 S. Khatun and P. Roy, *Chem. Commun.*, 2020, **56**, 7293–7296.